

Geometric criticality in the driven Jaynes-Cummings model

Ken Chen,¹ Jia-Hao Lü,¹ Hao-Long Zhang,¹ Fan Wu,¹ Wen Ning,^{1,*} Zhen-Biao Yang,^{1,2,†} and Shi-Biao Zheng^{1,2,‡}

¹*Fujian Key Laboratory of Quantum Information and Quantum Optics, College of Physics and Information Engineering, Fuzhou University, Fuzhou, Fujian 350108, China*

²*Hefei National Laboratory, Hefei 230088, China*

When the photonic mode in the Jaynes-Cummings model is driven by an external classical field, the system can undergo the photon-blockade breakdown phase transition at a critical point. Such a phase transition has been detailedly investigated, but the critical properties of the eigenstates remain largely unexplored so far. We here study the geometric criticality associated with these eigenstates. The amplitude and phase of the drive serve as the control parameter of the governing Hamiltonian. We find the quantum metric and Berry curvature tensors for each eigenstate display divergent behaviors in the critical region. More importantly, the divergence associated with bright eigenstates is much more pronounced than that for the unique dark state. Our theoretical results can be experimentally confirmed in circuit quantum electrodynamics systems, where the driven Jaynes-Cummings model has been realized.

I. INTRODUCTION

In recent years, increasing interest has been paid to quantum geometry [1–4], quantified by the quantum geometric tensor (QGT) [5], which describes the inherent geometry of the eigenstate space of the Hamiltonian governing the behaviors of a quantum state. The real part of the QGT, which is symmetric and referred to as quantum metric, measures the distance between nearby eigenstates of the Hamiltonian. The quantum metric plays a critical role in understanding important physical phenomena in solid-state physics, exemplified by flat-band superconductivity [4]. Its imaginary part, which is antisymmetric and known as Berry curvature [6], provides information about phase change of the eigenstates [3]. The integral of the Berry curvature over a closed manifold yields the Chern number, which quantifies the topology of the manifold. The Berry curvature can be thought as the fictitious magnetic field emanated by a topological monopole, and is responsible for intriguing electronic transport phenomena, e.g., quantum anomalous Hall effect [7–9]. In recent years, the QGT has been measured with different types of pseudospins, including NV centers in diamond [10], ultracold atoms [11], and superconducting qubits [12, 13], polariton systems [14], and Bloch electrons in solids [15].

Apart from laying the foundation for topological physics, the QGT provides a new insight to quantum phase transitions without resorting to order parameters [16–20]. In the proximity of a quantum phase transition, the eigenstates of the Hamiltonian undergo a dramatic change even if the control parameter is only slightly changed. As such, it is expected that the QGT associated with each eigenstate exhibits divergent behaviors

near the critical point. Such critical behaviors have been theoretically investigated in different systems, including the parametrically-driven nonlinear resonator [21], Dicke model [22], and parametrically-driven Tavis-Cummings model [23]. These systems bear a common feature that the Hamiltonian is symmetric under the parity transformation. The corresponding phase transition originates from the spontaneous parity breaking of the parity. Despite these theoretical advancements, experimental observations of the critical geometric phenomena are still lacking.

In this paper, we study the critical behaviors of entangled eigenstates of the driven Jaynes-Cummings model (JCM) [24–28], where photonic mode is coupled to a qubit and driven by an external classical field. This drive breaks the U(1) symmetry of the Jaynes-Cummings model. Neither does the driven Jaynes-Cummings model have the parity symmetry. Such a system possesses a unique dark eigenstate and infinitely many bright doublets. The quasienergy splittings of the doublets vanish after crossing the critical point, where the drive strength is equal to half of the coupling strength between the qubit and the photonic mode. The critical behavior of the qubit in the dark state has been exploited for realizing robust quantum metrology [28]. However, the critical geometric features have not been touched upon so far. We here investigate quantum geometry for such a critical system. The calculated quantum metric and Berry curvature for each eigenstate diverge at the critical point. The critical features associated with bright eigenstates are much stronger than those for the dark state. As neither the thermodynamical limit nor the scaling limit is required to observe the critical behaviors of the driven JCM, this is in distinct contrast with other qubit-photon systems [22, 29–31]. As such, our theoretical results can be experimentally demonstrated with presently available techniques, which would shed new light on critical phenomena in fully quantum-mechanical light-matter systems.

* ningw@fzu.edu.cn

† zbyang@fzu.edu.cn

‡ t96034@fzu.edu.cn

II. EIGENSTATES AND EIGENENERGIES OF THE DRIVEN JCM

We begin by considering the driven JCM [24, 32, 33], which describes a two-level system resonantly coupled to a quantum field mode while simultaneously driven by an on-resonance signal field. The interaction Hamiltonian in the interaction picture is given by ($\hbar = 1$ is set)

$$H = \Omega[a^\dagger|g\rangle\langle e| + a|e\rangle\langle g| + \eta(a^\dagger e^{-i\phi} + a e^{i\phi})/2], \quad (1)$$

where $|g\rangle$ and $|e\rangle$ are the ground and excited state of the two-level system, a^\dagger and a are the creation and annihilation operators for the quantized field mode, Ω represents the coupling strength, and η characterizes the rescaled amplitude of the driven field with the phase ϕ .

Next, we solve the eigenvalue problem with

$$H|\psi_E\rangle = E|\psi_E\rangle. \quad (2)$$

Here we expand the eigenstate as

$$|\psi_E\rangle = |\psi_E^+\rangle|e\rangle + |\psi_E^-\rangle|g\rangle, \quad (3)$$

where $|\psi_E^+\rangle$ and $|\psi_E^-\rangle$ are field states normalized, satisfying the condition of $\langle\psi_E|\psi_E\rangle = 1$. Therefore, the eigenvalue problem can be expressed as

$$\left[\frac{\Omega\eta}{2}(a^\dagger e^{-i\phi} + a e^{i\phi}) - E\right]|\psi_E^+\rangle + \Omega a |\psi_E^-\rangle = 0, \quad (4a)$$

$$\Omega a^\dagger |\psi_E^+\rangle + \left[\frac{\Omega\eta}{2}(a^\dagger e^{-i\phi} + a e^{i\phi}) - E\right]|\psi_E^-\rangle = 0. \quad (4b)$$

Here we multiply Eq. (4a) and Eq. (4b) on the left by a^\dagger and a , respectively, which gives rise to

$$\left\{ -\left[\frac{\eta}{2}(a^\dagger e^{-i\phi} + a e^{i\phi}) - \frac{E}{\Omega} \right]^2 + a^\dagger a \right\} |\psi_E^-\rangle - \frac{\eta}{2} e^{i\phi} |\psi_E^+\rangle = 0, \quad (5a)$$

$$\left\{ -\left[\frac{\eta}{2}(a^\dagger e^{-i\phi} + a e^{i\phi}) - \frac{E}{\Omega} \right]^2 + a a^\dagger \right\} |\psi_E^+\rangle + \frac{\eta}{2} e^{-i\phi} |\psi_E^-\rangle = 0. \quad (5b)$$

By combining Eq. (5a) and Eq. (5b), we obtain

$$\mathcal{A}_p(E)\mathcal{A}_m(E)|\psi_E^-\rangle = 0, \quad (6)$$

where

$$\mathcal{A}_p(E) = \mathcal{A}(E) + \frac{1}{2}\sqrt{1-\eta^2}, \quad (7a)$$

$$\mathcal{A}_m(E) = \mathcal{A}(E) - \frac{1}{2}\sqrt{1-\eta^2}, \quad (7b)$$

$$\mathcal{A}(E) = -\left[\frac{\eta}{2}(a^\dagger e^{-i\phi} + a e^{i\phi}) - \frac{E}{\Omega}\right]^2 + \frac{a^\dagger a + a a^\dagger}{2}, \quad (7c)$$

where $\mathcal{A}_p(E)$ and $\mathcal{A}_m(E)$ satisfy the commutation relation, i.e., $[\mathcal{A}_p(E), \mathcal{A}_m(E)] = 0$. Therefore, the general solution may be written as

$$|\psi_E^-\rangle = c_p |\psi_{E,p}^-\rangle + c_m |\psi_{E,m}^-\rangle, \quad (8)$$

where $|\psi_{E,p}^-\rangle$ and $|\psi_{E,m}^-\rangle$ are solutions to the equations

$$\mathcal{A}_p(E)|\psi_{E,p}^-\rangle = 0, \quad (9a)$$

$$\mathcal{A}_m(E)|\psi_{E,m}^-\rangle = 0. \quad (9b)$$

Using Eq. (5a) and Eqs. (7), we can write

$$|\psi_E^+\rangle = \left(\frac{\eta}{2}e^{i\phi}\right)^{-1}\{\mathcal{A}_{p,m} - \frac{1}{2}[1 \pm \sqrt{1-\eta^2}]\}|\psi_E^-\rangle, \quad (10)$$

where the \pm notation indicates two alternative forms with $+$ corresponding to the p-subscripted form and $-$ to the m-subscripted form. According to Eqs. (9) and Eq. (10), we have

$$|\psi_E^+\rangle = -(\eta e^{i\phi})^{-1}\{c_p[1 + \sqrt{1-\eta^2}]|\psi_{E,p}^-\rangle + c_m[1 - \sqrt{1-\eta^2}]|\psi_{E,m}^-\rangle\}. \quad (11)$$

To solve Eqs. (9), we use squeezing and displacement transformations to convert Eqs. (9) into eigenvalue equations for a harmonic oscillator. We multiply Eqs. (9) on the left by $D^\dagger(\alpha)S^\dagger(\xi)$ and transform the operators $\mathcal{A}_p(E)$ and $\mathcal{A}_m(E)$ using

$$D^\dagger(\alpha)aD(\alpha) = a + \alpha, \quad (12a)$$

$$S^\dagger(\xi)aS(\xi) = a \cosh r - a^\dagger e^{i\theta} \sinh r, \quad (12b)$$

where $D(\alpha) = e^{\alpha a^\dagger - \alpha^* a}$ and $S(\xi) = e^{-\frac{1}{2}(\xi a^\dagger)^2 - \xi^* a^2}$. So when we choose

$$\alpha = -\eta(1-\eta^2)^{-3/4}\frac{E}{\Omega}e^{-i\phi}, \quad (13a)$$

$$\xi = r e^{-2i\phi}, \quad r = \frac{1}{4}\ln(1-\eta^2), \quad (13b)$$

Eqs. (9) can be substituted by the following equations

$$a^\dagger a |\tilde{\psi}_{E,p}^-\rangle = \left[\left(\frac{E}{\Omega}\right)^2(1-\eta^2)^{-3/2} - 1\right] |\tilde{\psi}_{E,p}^-\rangle, \quad (14a)$$

$$a^\dagger a |\tilde{\psi}_{E,m}^-\rangle = \left(\frac{E}{\Omega}\right)^2(1-\eta^2)^{-3/2} |\tilde{\psi}_{E,m}^-\rangle, \quad (14b)$$

where $|\tilde{\psi}_{E,p}^-\rangle = D^\dagger(\alpha)S^\dagger(r)|\psi_{E,p}^-\rangle$ and $|\tilde{\psi}_{E,m}^-\rangle = D^\dagger(\alpha)S^\dagger(r)|\psi_{E,m}^-\rangle$.

The solutions of Eqs. (14) are Fock states if and only if the constants on the right-hand sides are restricted to the discrete set of non-negative integers. From Eqs. (14),

we obtain the discrete eigenenergies as

$$E_0 = 0, \quad (15a)$$

$$E_{n,\pm} = \pm \sqrt{n}\Omega(1 - \eta^2)^{3/4} \quad (n = 1, 2, \dots). \quad (15b)$$

The corresponding states are

$$|\tilde{\psi}_{E;p}^-\rangle = |n-1\rangle, \quad (n = 1, 2, \dots) \quad (16a)$$

$$|\tilde{\psi}_{E;m}^-\rangle = \begin{cases} |0\rangle \\ |n\rangle, \end{cases} \quad (n = 1, 2, \dots). \quad (16b)$$

Furthermore, we can obtain

$$|\psi_{E;p}^-\rangle = S(r)D(\alpha)|n-1\rangle = |r, \alpha, n-1\rangle, \quad (17a)$$

$$|\psi_{E;m}^-\rangle = \begin{cases} S(r)D(\alpha)|0\rangle \\ S(r)D(\alpha)|n\rangle \end{cases} = |r, \alpha, 0\rangle \quad (17b)$$

The ratio of constants c_p and c_m in Eq. (8) is determined by imposing the constraint from Eq. (4b), while their separate values are fixed through the normalization

$$\langle \psi_E | \psi_E \rangle = \langle \psi_E^+ | \psi_E^+ \rangle + \langle \psi_E^- | \psi_E^- \rangle = 1. \quad (18)$$

The calculation, while conceptually straightforward, involves considerable algebraic manipulation. We therefore present only the final results as follows

$$|\psi_0\rangle = S(\xi)|0\rangle|\phi_0\rangle, \quad (19a)$$

$$|\psi_{n,\pm}\rangle = S(\xi)D(\alpha_{n,\pm})(|n-1\rangle|\phi_1\rangle \pm |n\rangle|\phi_0\rangle)/\sqrt{2}, \quad (19b)$$

where $S(\xi)$ and $D(\alpha_{n,\pm})$ are the squeezing and displacement operators for the photonic field, respectively, with $\xi = \frac{1}{4}e^{-2i\phi} \ln(1 - \eta^2)$ and $\alpha_{n,\pm} = \mp\sqrt{n}\eta e^{-i\phi}$. The expressions of $|\phi_0\rangle$ and $|\phi_1\rangle$ are given by

$$|\phi_0\rangle = c_+|g\rangle - e^{-i\phi}c_-|e\rangle, \quad (20a)$$

$$|\phi_1\rangle = c_+|e\rangle - e^{i\phi}c_-|g\rangle, \quad (20b)$$

with $c_{\pm} = (1 \pm \sqrt{1 - \eta^2})^{1/2}/\sqrt{2}$.

III. CRITICAL QGT

Here, we apply the QGT to investigate the singular behavior of the driven JCM in the vicinity of the critical points. We consider a nondegenerate quantum state $|\psi(\lambda)\rangle$ in a parameter space spanned by N dimensionless parameters $\lambda(\lambda_1, \lambda_2, \dots, \lambda_N)$, the QGT is defined as [5]

$$\begin{aligned} Q_{\mu\nu} &= \langle \partial_{\mu}\psi(\lambda) | [1 - \mathcal{P}(\lambda)] | \partial_{\nu}\psi(\lambda) \rangle \\ &= \mathcal{G}_{\mu\nu} - \frac{i}{2}\mathcal{B}_{\mu\nu}, \end{aligned} \quad (21)$$

where $\{|\psi(\lambda)\rangle\}$ forms a complete orthonormal basis space and $\mathcal{P}(\lambda) = |\psi(\lambda)\rangle\langle\psi(\lambda)|$ is the Hilbert eigenspace pro-

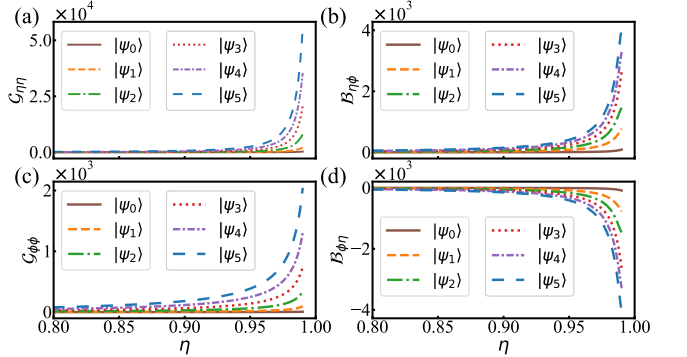


FIG. 1. The quantum metric $\mathcal{G}_{\eta\eta}$ (a), $\mathcal{G}_{\phi\phi}$ (c) and the Berry curvature $\mathcal{B}_{\eta\phi}$ (b), $\mathcal{B}_{\phi\eta}$ (d) with respect to η for $\phi = 0$. The eigenstates $|\psi_i\rangle$ ($i = 0, 1, 2, 3, 4, 5$) correspond to $n = 0, 1, 2, 3, 4, 5$, respectively. The quantum metric $\mathcal{G}_{\eta\phi}$, $\mathcal{G}_{\phi\eta}$ and the Berry curvature $\mathcal{B}_{\eta\eta}$, $\mathcal{B}_{\phi\phi}$ are equal to zero, and not shown here.

jection operator. Its real component defines the quantum metric, $\mathcal{G}_{\mu\nu} = \text{Re}\{Q_{\mu\nu}\} = \mathcal{G}_{\nu\mu}$, while imaginary component is related to the Berry curvature, $\mathcal{B}_{\mu\nu} = -2\text{Im}\{Q_{\mu\nu}\} = -\mathcal{B}_{\nu\mu}$.

A remarkable feature of the QGT is that its divergent behavior in the vicinity of the critical point [13, 19, 34]. To elucidate this behavior, we derive a perturbative expression for QGT. Substituting the identity operator $\mathbb{I} = \sum_m |\psi_m\rangle\langle\psi_m|$ into Eq. (21) and using

$$\langle \psi_m | \partial_{\nu}\psi_n \rangle = \frac{\langle \psi_m | \frac{\partial H}{\partial \nu} | \psi_n \rangle}{E_n - E_m} \quad (m \neq n), \quad (22)$$

which is determined by the eigenvalue equation $H|\psi_n\rangle = E_n|\psi_n\rangle$, we reformulate Eq. (21) as follows [35]:

$$Q_{n,\mu\nu} = \sum_{m \neq n} \frac{\langle \psi_n | \frac{\partial H}{\partial \mu} | \psi_m \rangle \langle \psi_m | \frac{\partial H}{\partial \nu} | \psi_n \rangle}{(E_m - E_n)^2}. \quad (23)$$

This expression confirms that the QGT components—the quantum metric tensor and Berry curvature—become singular at stationary points of the QPT, marked by ground-state level crossings.

We consider the QGT space formed by the parameters η and ϕ , as shown in Fig. 1. Fig. 1(a) and Fig. 1(c) show the real parts of the QGT, i.e., $\mathcal{G}_{\eta\eta}$ and $\mathcal{G}_{\phi\phi}$, with respect to η , over the ground state $|\psi_0\rangle$ and the forefront five low-lying excited states $|\psi_i\rangle$ ($i = 1, 2, 3, 4, 5$); while Fig. 1(b) and Fig. 1(d) show the imaginary parts of the QGT, i.e., $\mathcal{B}_{\eta\phi}$ and $\mathcal{B}_{\phi\eta}$, as the function of η , over the same states. It is clearly shown that, all $\mathcal{G}_{\eta\eta}$, $\mathcal{G}_{\phi\phi}$, $\mathcal{B}_{\eta\phi}$ and $\mathcal{B}_{\phi\eta}$, in the excited states $|\psi_i\rangle$ ($i = 1, 2, 3, 4, 5$), exhibit significantly greater divergence compared to the ground state $|\psi_0\rangle$. Furthermore, the behavior of the divergence becomes stronger as the energy level separation of $|\psi_i\rangle$ ($i = 1, 2, 3, 4, 5$) from $|\psi_0\rangle$ becomes larger, which can also be seen from Eq. (23).

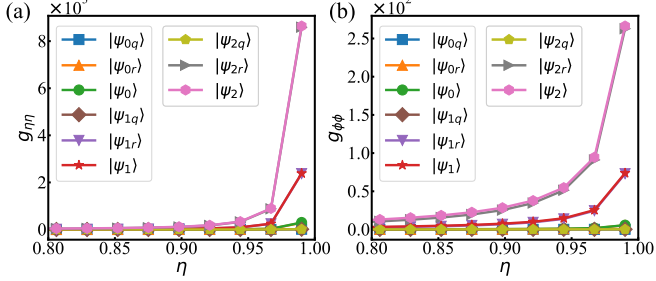


FIG. 2. The Bures metric $g_{\eta\eta}$ (a) and $g_{\phi\phi}$ (b) as a function of η . Here $|\psi_i\rangle$, $|\psi_{iq}\rangle$ and $|\psi_{ir}\rangle$ ($i = 0, 1, 2$) represent the eigenstates of the composite system, the two-level subsystem and the quantum field mode, respectively. The $g_{\eta\phi}$ and $g_{\phi\eta}$ are equal to zero, and not shown here.

In quantum information geometry, the Bures metric defines a natural Riemannian structure on the space of density matrices, which is derived from the Bures distance. For two density matrices ρ_1 and ρ_2 , the Bures distance is defined via the Uhlmann fidelity $\mathcal{F}(\rho_1, \rho_2) = (\text{tr} \sqrt{\sqrt{\rho_1} \rho_2 \sqrt{\rho_1}})^2$ [36] as

$$dS^2(\rho_1, \rho_2) = 2 \left(1 - \sqrt{\mathcal{F}(\rho_1, \rho_2)} \right). \quad (24)$$

The corresponding Bures metric g_{ij} is given by

$$\sum_{i,j} g_{ij}(\mathbf{x}) dx_i dx_j = dS^2(\rho_{\mathbf{x}}, \rho_{\mathbf{x}+\mathbf{dx}}), \quad (25)$$

which quantifies the distinguishability between two neighboring density matrices, $\rho_{\mathbf{x}}$ and $\rho_{\mathbf{x}+\mathbf{dx}}$, in a parameter space \mathbf{x} .

As shown in Fig. 2, the Bures metric components $g_{\eta\eta}$ and $g_{\phi\phi}$ become divergent in the proximity of the critical point. The eigenstates of the composite system are denoted by $|\psi_i\rangle$ ($i = 0, 1, 2$), which describe the product state of the eigenstates of the two-level subsystem ($|\psi_{iq}\rangle$) and the quantum field mode ($|\psi_{ir}\rangle$), i.e., $|\psi_i\rangle = |\psi_{iq}\rangle \otimes |\psi_{ir}\rangle$. Moreover, it is shown that Bures metric components $g_{\eta\eta}$ and $g_{\phi\phi}$ diverge much more strongly in the excited states $|\psi_i\rangle$ ($i = 1, 2$) than in the ground state $|\psi_0\rangle$. Interestingly, this divergent behavior is monotonically enhanced as the energy-level distance of $|\psi_i\rangle$ ($i = 1, 2$) from the ground state $|\psi_0\rangle$ increases. It's noted that the Bures metric components $g_{\eta\eta}$ and $g_{\phi\phi}$ of the composite system are dominated by contributions from the quantum field mode eigenstates $|\psi_{ir}\rangle$ ($i = 0, 1, 2$).

IV. EXPERIMENTAL FEASIBILITY

The difficulty in the experimental preparation of a target quantum state stems from the fact that, although it is theoretically well-defined, its direct initialization is

often prohibitively challenging. To circumvent this, a widely employed strategy leverages the quantum adiabatic theorem [28, 37–41]. Such an approach initializes the system in an easily preparable eigenstate at an initial parameter value, subsequently applying a slow, continuous drive to evolve the Hamiltonian towards the final parameter value. Within our framework, the dynamics of the driven JCM can be governed by the time-dependent critical parameter $\eta = \sqrt{1 - [(kt)^{4/3} + 1]^{-1}}$ [26], where k determines the ramping velocity. Initial conditions at $t = 0$ are set to $|\psi\rangle$ for the ground state and to the superposition state $(|n-1\rangle|e\rangle \pm |n\rangle|g\rangle)/\sqrt{2}$ for the i th eigenstates, respectively.

However, the experimental feasibility of this approach is fundamentally constrained by the adiabatic condition, which requires that the driving rate ($\sim 1/t$, t is the evolution time) be much smaller relative to the spectral gaps along the parameter trajectory [42, 43]. This requirement becomes particularly stringent near quantum critical regions, where the protocol's driving speed must be drastically reduced. Notably, the requisite slow-down is even more pronounced for the excited states. This substantial prolongation of adiabatic evolution time introduces a fundamental limitation for implementing robust quantum information protocols under realistic experimental conditions. To overcome this challenge, a possible solution resorts to so-called counterdiabatic driving, which is also known as the adiabatic shortcut [44–47]. By introducing auxiliary control fields that actively suppress non-adiabatic excitations, it enables, in principle, a transitionless quantum evolution within an arbitrarily short duration, offering a pathway toward robust finite-time quantum state engineering in critical systems. Furthermore, a recent study has demonstrated an excited state preparation technique that exploits the physical coupling between photons and electrons to directly convert between ground and excited states [48].

V. CONCLUSIONS

In conclusion, we have studied the quantum geometry associated with the eigenstates of the driven JCM. Our results reveal that both the quantum metric and Berry curvature exhibit critical behaviors near the photon-blockade breakdown phase transition. The divergent features of these quantum geometric properties for bright eigenstates are much more pronounced than those for the dark eigenstate. Our work provides a direct insight into critical phenomena in fully quantum-mechanical light-matter systems from the view of differential geometry. The predicted geometric features can be observed with present techniques in superconducting circuits.

VI. ACKNOWLEDGEMENTS

This work was supported by the National Natural Science Foundation of China (Grants No. 12474356, No. 12475015, No. 12274080, No. 12505016), and the Natural Science Foundation of Fujian Province (Grant No. 2025J01465).

[1] P. Törmä, S. Peotta, and B. A. Bernevig, Superconductivity, superfluidity and quantum geometry in twisted multilayer systems, *Nat. Rev. Phys.* **4**, 528 (2022).

[2] S. Peotta, K.-E. Huhtinen, and P. Törmä, Quantum geometry in superfluidity and superconductivity, *Proc. Int. Sch. Phys. “Enrico Fermi”* **211**, 373–404 (2025).

[3] P. Törmä, Essay: Where can quantum geometry lead us?, *Phys. Rev. Lett.* **131**, 240001 (2023).

[4] T. Liu, X.-B. Qiang, H.-Z. Lu, and X. C. Xie, Quantum geometry in condensed matter, *Natl. Sci. Rev.* **12**, nwaee334 (2024).

[5] J. P. Provost and G. Vallee, Riemannian structure on manifolds of quantum states, *Commun. Math. Phys.* **76**, 289 (1980).

[6] M. V. Berry, Quantal phase factors accompanying adiabatic changes, *Proc. R. Soc. Lond. A* **392**, 45 (1984).

[7] R. Yu, W. Zhang, H.-J. Zhang, S.-C. Zhang, X. Dai, and Z. Fang, Quantized anomalous Hall effect in magnetic topological insulators, *Science* **329**, 61 (2010).

[8] C.-Z. Chang, J. Zhang, X. Feng, J. Shen, Z. Zhang, *et al.*, Experimental observation of the quantum anomalous Hall effect in a magnetic topological insulator, *Science* **340**, 167 (2013).

[9] J. G. Checkelsky, R. Yoshimi, A. Tsukazaki, K. S. Takahashi, Y. Kozuka, J. Falson, M. Kawasaki, and Y. Tokura, Trajectory of the anomalous Hall effect towards the quantized state in a ferromagnetic topological insulator, *Nat. Phys.* **10**, 731 (2014).

[10] M. Yu, P. Yang, M. Gong, Q. Cao, Q. Lu, H. Liu, S. Zhang, M. B. Plenio, F. Jelezko, T. Ozawa, N. Goldman, and J. Cai, Experimental measurement of the quantum geometric tensor using coupled qubits in diamond, *Natl. Sci. Rev.* **7**, 254 (2020).

[11] M. Chen, C. Li, G. Palumbo, Y.-Q. Zhu, N. Goldman, and P. Cappellaro, A synthetic monopole source of Kalb-Ramond field in diamond, *Science* **375**, 1017 (2022).

[12] P. Roushan, C. Neill, Y. Chen, M. Kolodrubetz, C. Quintana, *et al.*, Observation of topological transitions in interacting quantum circuits, *Nature* **515**, 241 (2014).

[13] X. Tan, D.-W. Zhang, Z. Yang, J. Chu, Y.-Q. Zhu, D. Li, X. Yang, S. Song, Z. Han, Z. Li, Y. Dong, H.-F. Yu, H. Yan, S.-L. Zhu, and Y. Yu, Experimental measurement of the quantum metric tensor and related topological phase transition with a superconducting qubit, *Phys. Rev. Lett.* **122**, 210401 (2019).

[14] N. Fläschner, B. S. Rem, M. Tarnowski, D. Vogel, D.-S. Lühmann, K. Sengstock, and C. Weitenberg, Experimental reconstruction of the Berry curvature in a Floquet Bloch band, *Science* **352**, 1091 (2016).

[15] A. Gianfrate, O. Bleu, L. Dominici, V. Ardizzone, M. De Giorgi, D. Ballarini, G. Lerario, K. W. West, L. N. Pfeiffer, D. D. Solnyshkov, D. Sanvitto, and G. Malpuech, Measurement of the quantum geometric tensor and of the anomalous Hall drift, *Nature* **578**, 381 (2020).

[16] S. Kim, Y. Chung, Y. Qian, S. Park, C. Jozwiak, E. Rotenberg, A. Bostwick, K. S. Kim, and B.-J. Yang, Direct measurement of the quantum metric tensor in solids, *Science* **388**, 1050 (2025).

[17] Q. Liao, C. Leblanc, J. Ren, F. Li, Y. Li, D. Solnyshkov, G. Malpuech, J. Yao, and H. Fu, Experimental measurement of the divergent quantum metric of an exceptional point, *Phys. Rev. Lett.* **127**, 107402 (2021).

[18] P. Zanardi, P. Giorda, and M. Cozzini, Information-theoretic differential geometry of quantum phase transitions, *Phys. Rev. Lett.* **99**, 100603 (2007).

[19] L. Campos Venuti and P. Zanardi, Quantum critical scaling of the geometric tensors, *Phys. Rev. Lett.* **99**, 095701 (2007).

[20] A. T. Rezakhani, D. F. Abasto, D. A. Lidar, and P. Zanardi, Intrinsic geometry of quantum adiabatic evolution and quantum phase transitions, *Phys. Rev. A* **82**, 012321 (2010).

[21] H.-L. Zhang, J.-H. Lü, K. Chen, X.-J. Yu, F. Wu, Z.-B. Yang, and S.-B. Zheng, Critical quantum geometric tensors of parametrically-driven nonlinear resonators, *Opt. Express* **32**, 22566 (2024).

[22] X. Zhu, J.-H. Lü, W. Ning, L.-T. Shen, F. Wu, and Z.-B. Yang, Quantum geometric tensor and critical metrology in the anisotropic Dicke model, *Phys. Rev. A* **109**, 052621 (2024).

[23] J.-H. Lü, P.-R. Han, W. Ning, X. Zhu, F. Wu, L.-T. Shen, Z.-B. Yang, and S.-B. Zheng, Quantum metric and metrology with parametrically-driven Tavis-Cummings models, *Opt. Express* **31**, 41669 (2023).

[24] P. Alsing, D.-S. Guo, and H. J. Carmichael, Dynamic stark effect for the Jaynes-Cummings system, *Phys. Rev. A* **45**, 5135 (1992).

[25] H. J. Carmichael, Breakdown of photon blockade: A dissipative quantum phase transition in Zero dimensions, *Phys. Rev. X* **5**, 031028 (2015).

[26] J. B. Curtis, I. Boettcher, J. T. Young, M. F. Maghrebi, H. Carmichael, A. V. Gorshkov, and M. Foss-Feig, Critical theory for the breakdown of photon blockade, *Phys. Rev. Res.* **3**, 023062 (2021).

[27] J. M. Fink, A. Dombi, A. Vukics, A. Wallraff, and P. Domokos, Observation of the photon-blockade breakdown phase transition, *Phys. Rev. X* **7**, 011012 (2017).

[28] J.-H. Lü, W. Ning, F. Wu, R.-H. Zheng, K. Chen, X. Zhu, Z.-B. Yang, H.-Z. Wu, and S.-B. Zheng, Critical quantum metrology robust against dissipation and nonadiabaticity, *Sci. Adv.* **12**, eady2358 (2026).

[29] N. Lambert, C. Emary, and T. Brandes, Entanglement and the phase transition in single-mode superradiance, *Phys. Rev. Lett.* **92**, 073602 (2004).

- [30] S. Ashhab, Superradiance transition in a system with a single qubit and a single oscillator, *Phys. Rev. A* **87**, 013826 (2013).
- [31] M.-J. Hwang, R. Puebla, and M. B. Plenio, Quantum phase transition and universal dynamics in the Rabi model, *Phys. Rev. Lett.* **115**, 180404 (2015).
- [32] S. M. Dutra, P. L. Knight, and H. Moya-Cessa, Large-scale fluctuations in the driven Jaynes-Cummings model, *Phys. Rev. A* **49**, 1993 (1994).
- [33] M. Feng, Y. Zhong, T. Liu, L. Yan, W. Yang, J. Twamley, and H. Wang, Exploring the quantum critical behaviour in a driven Tavis-Cummings circuit, *Nat. Commun.* **6**, 7111 (2015).
- [34] D. Gutiérrez-Ruiz, D. Gonzalez, J. Chávez-Carlos, J. G. Hirsch, and J. D. Vergara, Quantum geometric tensor and quantum phase transitions in the Lipkin-Meshkov-Glick model, *Phys. Rev. B* **103**, 174104 (2021).
- [35] S.-J. GU, Fidelity approach to quantum phase transitions, *Int. J. Mod. Phys. B* **24**, 4371 (2010).
- [36] A. Uhlmann, The “transition probability” in the state space of a * -algebra, *Rep. Math. Phys.* **9**, 273 (1976).
- [37] T. Albash and D. A. Lidar, Adiabatic quantum computation, *Rev. Mod. Phys.* **90**, 015002 (2018).
- [38] E. Farhi, J. Goldstone, S. Gutmann, and M. Sipser, Quantum computation by adiabatic evolution, [arXiv:quant-ph/0001106](https://arxiv.org/abs/quant-ph/0001106) (2000).
- [39] M. Born and V. Fock, Beweis des Adiabatensatzes, *Z. Physik* **51**, 165 (1928).
- [40] T. Kato, On the adiabatic theorem of quantum mechanics, *J. Phys. Soc. Jpn.* **5**, 435 (1950).
- [41] M. S. Sarandy and D. A. Lidar, Adiabatic approximation in open quantum systems, *Phys. Rev. A* **71**, 012331 (2005).
- [42] A. Polkovnikov, K. Sengupta, A. Silva, and M. Vengalattore, Colloquium: Nonequilibrium dynamics of closed interacting quantum systems, *Rev. Mod. Phys.* **83**, 863 (2011).
- [43] M. Kolodrubetz, D. Sels, P. Mehta, and A. Polkovnikov, Geometry and non-adiabatic response in quantum and classical systems, *Phys. Rep.* **697**, 1 (2017).
- [44] A. del Campo, Shortcuts to adiabaticity by counterdiabatic driving, *Phys. Rev. Lett.* **111**, 100502 (2013).
- [45] D. Sels and A. Polkovnikov, Minimizing irreversible losses in quantum systems by local counterdiabatic driving, *Proc. Natl. Acad. Sci. U.S.A.* **114**, E3909 (2017).
- [46] J. R. Finžgar, S. Notarnicola, M. Cain, M. D. Lukin, and D. Sels, Counterdiabatic driving with performance guarantees, *Phys. Rev. Lett.* **135**, 180602 (2025).
- [47] S. Morawetz and A. Polkovnikov, Universal counterdiabatic driving in Krylov space, *PRX Quantum* **6**, 040320 (2025).
- [48] H. G. A. Burton and M.-A. Filip, Excited state preparation on a quantum computer through adiabatic light-matter coupling, [arXiv:2511.22324](https://arxiv.org/abs/2511.22324) (2025).